Analytica Chimica Acta 766 (2013) 77–82

Contents lists available at SciVerse ScienceDirect

Analytica Chimica Acta

journal homepage: www.elsevier.com/locate/aca

Coffee-ring effects in laser desorption/ionization mass spectrometry

Jie-Bi Hu, Yu-Chie Chen*, Pawel L. Urban*

Department of Applied Chemistry, National Chiao Tung University, 1001 University Rd, Hsinchu, 300, Taiwan

HIGHLIGHTS

- Coffee rings occur during sample preparation for MALDI-MS and LDI-MS.
- They partly contribute to chemical heterogeneity of sample deposits.
- Coffee rings may be hidden within sample spots.
- Occurrence of coffee rings permits partial separation of sample components.
- In some cases, formation of coffee rings can be suppressed during sample preparation.

GRAPHICAL ABSTRACT

ARTICLE INFO

Article history:
Received 16 October 2012
Received in revised form
14 December 2012
Accepted 21 December 2012
Available online 3 January 2013

Keywords:
Coffee-ring effect
Matrix-assisted laser desorption/ionization
Mass spectrometry
Surface-assisted laser desorption/ionization
sample preparation
laser desorption/ionization

ABSTRACT

This report focuses on the heterogeneous distribution of small molecules (*e.g.* metabolites) within dry deposits of suspensions and solutions of inorganic and organic compounds with implications for chemical analysis of small molecules by laser desorption/ionization (LDI) mass spectrometry (MS). Taking advantage of the imaging capabilities of a modern mass spectrometer, we have investigated the occurrence of "coffee rings" in matrix-assisted laser desorption/ionization (MALDI) and surface-assisted laser desorption/ionization (SALDI) sample spots. It is seen that the "coffee-ring effect" in MALDI/SALDI samples can be both beneficial and disadvantageous. For example, formation of the coffee rings gives rise to heterogeneous distribution of analytes and matrices, thus compromising analytical performance and reproducibility of the mass spectrometric analysis. On the other hand, the coffee-ring effect can also be advantageous because it enables partial separation of analytes from some of the interfering molecules present in the sample. We report a "hidden coffee-ring effect" where under certain conditions the sample/matrix deposit appears relatively homogeneous when inspected by optical microscopy. Even in such cases, hidden coffee rings can still be found by implementing the MALDI-MS imaging technique. We have also found that to some extent, the coffee-ring effect can be suppressed during SALDI sample preparation.

1. Introduction

Matrix-assisted laser desorption/ionization (MALDI) [1] and surface-assisted laser desorption/ionization (SALDI) [2] facilitate detection of a wide range of analytes – from biomolecules to synthetic polymers – with high sensitivity [3–5]; therefore, they have become important ionization techniques used in mass spectrometric (MS) analysis during the past two decades. It is known that sample preparation protocols strongly influence the quality of MALDI and SALDI mass spectra. It has been widely discussed that the quality of MALDI-MS results is highly dependent on the quality of sample deposits on MALDI targets. Numerous sample preparation methods have been developed in order to improve homogeneity of crystalline sample deposits. Examples include electrospray-aided sample/matrix deposition [6], application of ionic-liquid matrices [7–9] as well as solvent-free methods [10,11]. Nevertheless, one of the "classical" and most widely used sample

* Corresponding authors. Tel.: +886 3 5731786; fax: +886 3 5723764.
E-mail addresses: yuchie@mail.nctu.edu.tw (Y.-C. Chen), plurban@nctu.edu.tw (P.L. Urban).

0003-2670/$ – see front matter © 2013 Elsevier B.V. All rights reserved.
http://dx.doi.org/10.1016/j.aca.2012.12.044

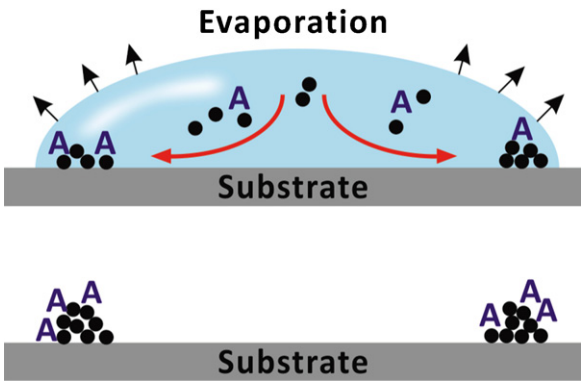

Fig. 1. Proposed directed self-organization of particles and analytes by coffee-ring effect in an evaporating droplet on a hydrophilic surface. Red arrow: outward capillary force; black particle: inorganic matrix; A: analyte species. Ideogram based on the model described by Bhardwaj et al. [59]. (For interpretation of the references to color in this figure legend, the reader is referred to the web version of the article.)

preparation methods is the so-called "dried-droplet method": a matrix solution is mixed with the sample directly on the surface of the MS target, which is then followed by the evaporation of the matrix and sample solvents under ambient conditions [12]. This method is easy to implement, and it can readily be used for the preparation of samples containing high amounts of salts and other components [13]. For example, it has been used in the direct profiling of complex mixtures, including crude extracts, cultures of bacteria, cell lysates, intact viruses, and even individual neurons [14]. Unfortunately, heterogeneity of the resulting sample spots usually leads to poor shot-to-shot and unsatisfactory sample-to-sample reproducibility of the MS signals. This method also necessitates searching for the so-called "sweet-spots" – microscale locations within the sample deposits that contain an elevated concentration of analyte molecules [15].

The occurrence of "sweet spots" is a major drawback of the sample preparation for MALDI, and it hampers the use of MALDI-MS for quantitative analysis. In many cases, one can also observe ring-like patterns formed at the perimeter of the sample spots; these rings can be attributed to the so-called "coffee-ring effect" [16]. The ring pattern formation is due to the action of capillary flow, which carries the solute and/or suspended non-volatile particles to the perimeter of the droplet [17]. Particles suspended in the drying droplet accumulate at the perimeter and form a circular ring pattern, as opposed to a uniform spot (Fig. 1). In fact, the coffee-ring effect has serious implications for many consumer products, such as inkjet printing [18], and coating polymers [19], as well as research techniques, such as microarray technology [20], chromatography [21,22], and structural analysis by transmission electron microscopy [23]. Therefore, the coffee-ring effect has been broadly studied by scientists in various fields.

One possibility for improving the sample spot homogeneity is using inorganic powder (micro- and nano-particles), such as graphite particles [2], carbon powder [24,25], and metal oxide powder [26–29] as matrices for facilitating ionization of the analytes of interest. In fact, inorganic material-aided SALDI-MS analysis has the advantage that sample preparation does not rely on the crystallization of an organic matrix compound; it can be used to concentrate analytes based on affinity interactions [25,30–36] and generally produces spectra with less noise in the low *m/z* range. To date, various nanomaterials (*e.g.* carbon nanotubes [35,36], porous silicon and silicon nanoparticles [37,38], TiO_2 [39–41], Fe_3O_4/TiO_2 [33], and gold nanoparticles [42,43]) have been proposed as possible assisting materials for SALDI-MS. Nevertheless, Kawasaki et al. found that dry deposits of gold nanoparticle suspensions also exhibit formation of the "coffee rings" following their deposition on target plates [44]. Alternatively, MALDI matrices – covalently immobilized on a sol–gel film – have been used to improve shot-to-shot reproducibility and eliminate background ions in the low *m/z* region [45–48]. Segregation of analytes in MALDI spots was observed using high-resolution MS imaging methods [49,50].

In the present paper, we discuss the occurrence of the coffee-ring effect during the sample preparation for analysis by MALDI-MS and SALDI-MS. We have implemented laser desorption/ionization imaging in order to study the formation of coffee rings in dry deposits of samples containing either organic or inorganic materials. We will show that although the coffee-ring effect can generally be considered as a nuisance in sample preparation for MALDI and SALDI, it also enables rough separation of sample components, which can be beneficial.

2. Materials and methods

2.1. Sample preparation

The dried-droplet sample preparation method was used in this study. For MALDI, 9-aminoacridine (9-AA) was used as matrix while for SALDI, 2-μm graphite powder and fluorescent platinum nanoclusters were used as SALDI-assisting materials. In each case, a 0.2-μL sample was premixed with 0.2 μL of the matrix cocktail in a microcentrifuge test tube, and the resulting mixture was deposited on various targets: glass substrate coated with an indium tin oxide (ITO) layer (ITO thickness: 260 ± 20 nm; resistivity: ~7 Ω cm; light transmission: ≥80%), ITO glass slides coated with a layer of polysilazane, or on a commercial disposable AnchorChip target (PAC II 384/96, CHCA prespotted on conductive polymer; Bruker Daltonics/Eppendorf, Bremen, Germany). In the case of the commercial disposable target, acetone and isopropanol were used to remove CHCA before experiments. Subsequently, the samples were dried at room temperature.

2.2. Synthesis and purification of fluorescent platinum nanoclusters

The fluorescent platinum nanoclusters (PtNCs) were synthesized as described previously [51]. Briefly, 150 μL of an aqueous 0.1-M H_2PtCl_6 solution was mixed with 15 mL of *N,N*-dimethylformamide (DMF) pre-heated to 140 °C, and the resulting mixture was refluxed in a 140 °C oil bath with vigorous stirring in ambient air for 8 h. Then, the as-prepared PtNCs were purified using prefilled ion exchange columns (Poly-Prep, AG 1-X8 resin, 200–400 mesh; BioRad, Hercules, CA, USA) to remove residual chloride ions and thus decrease spectral interferences caused by these species.

2.3. MALDI/SALDI imaging

All the MS measurements and MS imaging were conducted by means of the Autoflex III Smartbeam MALDI-MS instrument (Bruker Daltonics, Bremen, Germany), equipped with a solid-state laser (λ = 355 nm), and operated in the reflectron mode. During MS imaging, the laser beam was focused to a spot with a diameter between 60 and 70 μm; the default spacing of the scan raster was set to 100 μm; 100 laser shots were fired at each raster point with the preset frequency of 100 Hz. The mass range was normally set to 100–1000 Da and all the ions up to 100 Da were excluded in order to prevent saturation of the microchannel plate detector. Various standard compounds were spotted on the targets next to the sample spots, and used for mass calibration prior to the MS imaging scan.

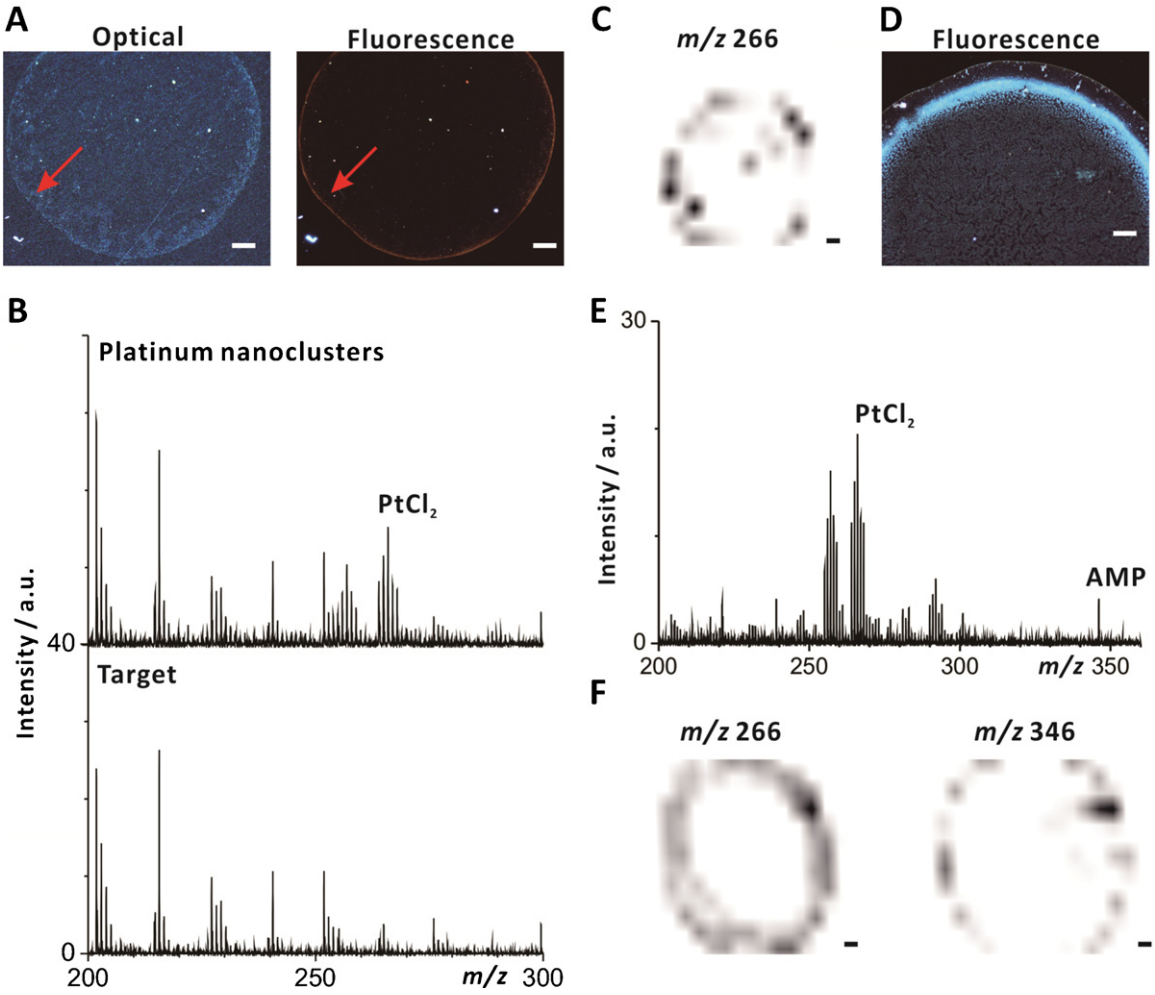

Fig. 2. Coffee-ring effect in SALDI-MS. (A) Optical and fluorescence (λ_{ex} = 330–380 nm; λ_{em} > 420 nm) images of dry spots composed of sub-nanometer fluorescent platinum nanoclusters on a commercial disposable AnchorChip target (no organic matrix present). (B) SALDI-MS spectra of platinum nanoclusters deposited on a commercial disposable AnchorChip target obtained in the negative-ion mode. (C) SALDI-MS image of platinum nanoclusters acquired in the negative-ion mode. (D) Fluorescence (λ_{ex} = 330–380 nm; λ_{em} > 420 nm) image of a spot containing AMP and platinum nanoclusters. (E) SALDI-MS spectrum of a spot containing AMP and platinum nanoclusters (negative-ion mode). (F) SALDI-MS images of a spot containing AMP and platinum nanoclusters (negative-ion mode). Laser spot diameter: 60–70 μm; laser raster spacing: 100 μm. Scale bars: 100 μm. Gray scale is used as a relative measure of the MS signal intensity. The red arrow highlights the edge of the spot. (For interpretation of the references to color in this figure legend, the reader is referred to the web version of the article.)

3. Results and discussion

In this present work, we investigate the formation of coffee rings during sample preparation for SALDI and MALDI mass spectrometry. The study starts with testing the influence of inorganic matrices (micro- and nano-particles) on the emergence of the coffee-ring effect, and continues with the investigation of "hidden coffee rings" in the deposits of an organic MALDI matrix.

3.1. Coffee rings in SALDI spots

For the initial tests we chose graphite powder (particle size: ~2 μm) as a model SALDI-assisting material [2]. This material is chemically inert, conducts electricity, and absorbs energy delivered by UV laser; therefore, it has been widely used in SALDI [2,52,53]. Conventionally, graphite powder is used at a high concentration (≥4 mg mL^{-1}), in which case sample deposits appear homogeneous, and high sensitivity is seen [54]. In order to observe the appearance of coffee rings during sample preparation for SALDI-MS, we used a suspension of graphite powder at a relatively low concentration (2.5 mg mL^{-1}). In Figure S1 one can see that most graphite particles accumulated in the rim of the spot following the evaporation of solvent. Several larger particles of graphite also accumulated in the central part of the spot, which gave rise to heterogeneous distribution of the graphite matrix. This effect can also be observed in SALDI-MS images which display the occurrence of carbon cluster ions (C_6^+ at *m/z* 72, C_8^+ at *m/z* 96, and C_{10}^+ at *m/z* 120) while scanning the surface of the spot with the UV laser (Figure S1).

In order to verify how particle size contributes to the coffee-ring effect, we further tested sub-nanometer fluorescent platinum nanoclusters (Figure S2) as the matrix material. To study the coffee-ring effect characteristics within dry nanocluster spots, we took advantage of various analytical techniques: optical/fluorescence microscopy, SALDI imaging, scanning electron microscopy (SEM), and energy-dispersive X-ray spectroscopy (EDX). Fig. 2A shows optical and fluorescent micrographs of ring-like patterns formed by platinum nanoclusters (~10 mg mL^{-1}, 0.2 μL). In order to investigate the distribution of platinum nanoclusters within dry spots, we executed SALDI-MS imaging sequences. In both positive and negative modes, ring-like patterns were revealed. In the negative-ion mode (Fig. 2B and C), we recorded MS signals corresponding to a $PtCl_2^-$ ion (*m/z* 266). In the positive-ion mode (Figure S3), we recorded two unknown signals (*m/z* 438 and 454), which were most abundant when the rim of the spot was scanned with the UV laser.

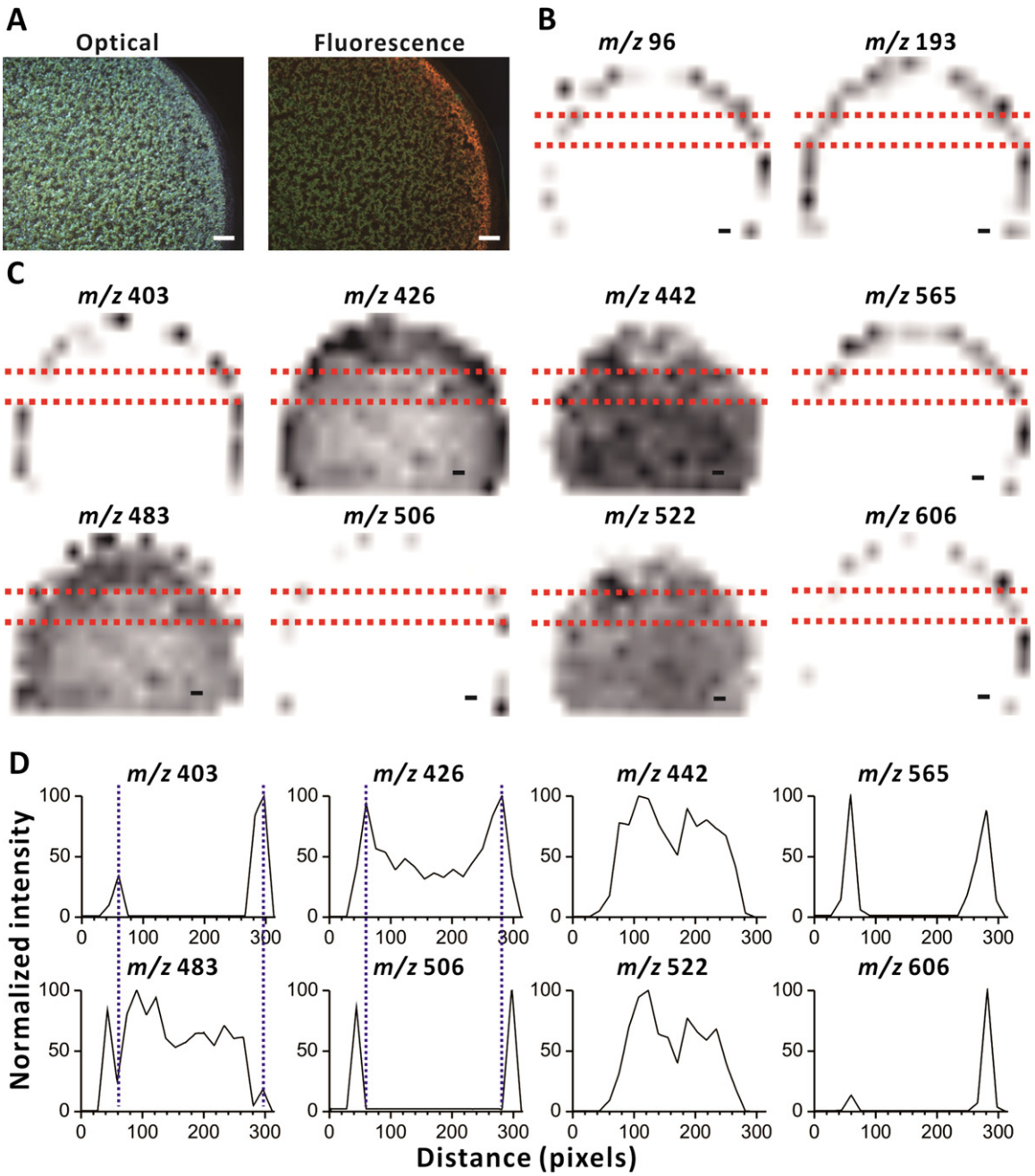

Fig. 3. Coffee-ring effect in MALDI-MS. (A) Optical and fluorescence (λ_{ex} = 330–380 nm; λ_{em} > 420 nm) images of a sample deposit containing various metabolite standards co-crystallized with the 9-aminoacridine matrix (9 mg mL^{-1}, 0.2 μL) prepared in acetone solvent. (B) MALDI-MS images corresponding to the species related to the 9-aminoacridine matrix. (C) MALDI-MS images corresponding to the metabolite standards. Signal assignment: *m/z* 403, uridine diphosphate; *m/z* 426, adenosine diphosphate; *m/z* 442, guanosine diphosphate; *m/z* 483, uridine triphosphate; *m/z* 506, adenosine triphosphate; *m/z* 522, guanosine triphosphate; *m/z* 565, uridine diphosphate glucose; *m/z* 606, uridine diphosphate *N*-acetylglucosamine. In all the MALDI-MS images the minimum (threshold) intensity was set to 60% (relative to the base peak). (D) Signal intensity profiles corresponding to MALDI-MS images in (C). Laser spot diameter: 60–70 μm; laser raster spacing: 100 μm. Scale bars: 100 μm. The gray scale is used as a relative measure of the MS signal intensity.

When analyzing the deposits of platinum nanoclusters by SEM and SEM-EDX, we confirmed that most platinum nanoclusters were localized within the rim zone of the spot while only a small portion of platinum nanoclusters was present near the center of the spot (Figure S4). This result is in agreement with the report by Kawasaki et al. on the use of nanomaterials as SALDI matrices [44]. Based on the authors' experience, the coffee rings are especially prominent at relatively low particle densities. Higher particle density will effectively reduce the occurrence of the coffee rings. Nonetheless, in many cases it is not possible to obtain concentrated suspensions of some of the novel SALDI-assisting materials.

The following analysis focused on the influence of the coffee-ring effect on the distribution of test analytes. We used adenosine monophosphate (AMP) as a test analyte. As shown in Fig. 2D and F, fluorescence micrographs and SALDI-MS images reveal $PtCl_2^-$ ions and the ions related to the analyte AMP when the laser light beam impinged on the rim zone. When AMP and bradykinin samples were deposited on the target without adding any matrix, coffee rings were observed (Figure S5). Therefore, the occurrence of the coffee-ring effect in SALDI-MS images, as seen in Fig. 2F, can be due to either accumulation of nanoclusters at the rim of the spot, accumulation

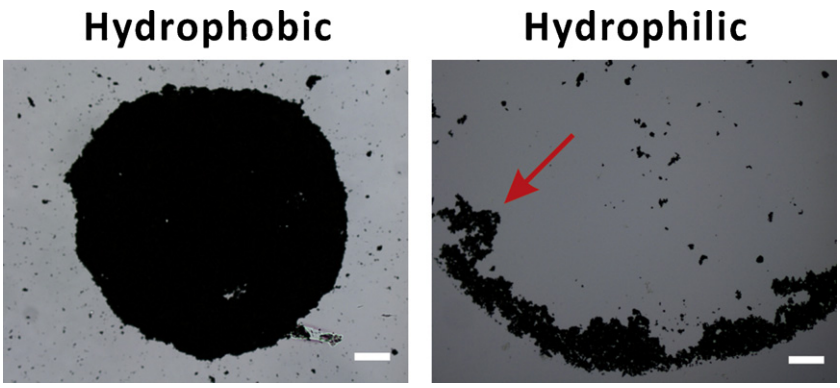

Fig. 4. The influence of surface wettability on the emergence of coffee rings. A spot of graphite powder suspension (2.5 mg mL^{-1}, 0.4 μL) deposited onto hydrophobic (left) and hydrophilic (right) surface. The arrow highlights the edge of the spot. Scale bars: 100 μm.

of the analyte molecules, or a combination of these two effects.

The solutes precipitating from homogeneous solutions (*e.g.* small molecules such as AMP) are also responsible for the formation of coffee rings. This observation is relevant to SALDI-MS variants which use micro- or nano-particles as SALDI-assisting materials. There has been considerable interest in the utilization of nanostructured surfaces for matrix-free MS (*e.g.* Refs. [37,55]); however, since the analytes themselves give rise to coffee rings (Figure S5), it cannot be taken for granted that the implementation of such surfaces can always provide homogeneous sample deposits.

3.2. Coffee rings in MALDI spots

We have further studied heterogeneous distribution of small molecules within crystalline deposits of an organic MALDI matrix by means of MALDI-MS imaging (Fig. 3A). We recorded signals of ions corresponding to the 9-aminoacridine matrix fragment (*m/z* 96 and 193; Fig. 3B) and the ions corresponding to the small-molecule analytes present in the sample (uridine diphosphate (*m/z* 403), adenosine diphosphate (*m/z* 426), uridine triphosphate (*m/z* 483), adenosine triphosphate (*m/z* 506), uridine diphosphate glucose (*m/z* 565), and uridine diphosphate *N*-acetylglucosamine (*m/z* 606); Fig. 3C). While some of these signals were relatively high when the laser beam impinged on the rim zone of the spot, other signals represented a uniform distribution within the spot. This can easily be judged based on the plots showing the signal intensity along an intersecting line drawn across the MALDI image of the spot (Fig. 3D). In particular, the signals of guanosine diphosphate (*m/z* 442) and guanosine triphosphate (*m/z* 522) were higher in the center of the spot, while the signals of uridine diphosphate (*m/z* 403), uridine triphosphate (*m/z* 483), adenosine diphosphate (*m/z* 426), and adenosine triphosphate (*m/z* 506) were relatively higher near the droplet periphery. This occurred even though the sample/matrix crystal appeared homogeneous when inspected by optical microscopy. Therefore, we conclude that separation of species occurred within the MALDI spot. The apparent separation of species within the spot (Fig. 3C and D) can be explained with various putative causes, for example: different solubilities of analytes, different concentrations of matrix on the target, interaction between analyte molecules and the matrix, or suppression/enhancement effects due to the heterogeneous distribution of inorganic ions. In fact, a zonal distribution of ionogenic species, which do not give rise to signals during analysis by MALDI-MS, may also contribute to the apparent separation of analyte species within the spots. It should be pointed out that the observed effect is especially clear because the intensity threshold used in the image display was set to 60% relative to the intensity of the base peak within the *m/z* range used (50–800 Da). The high threshold was chosen in order to highlight the differences in relative intensities between the edge and the center of MALDI spots. Interestingly, by implementing the MALDI imaging technique, a hidden coffee-ring effect could be observed (Fig. 3B and C), which is not evident from the optical images (Fig. 3A). While the current study focuses on the formation of rings in the MALDI spot peripheries, it should be noted that previous studies (using high-resolution MALDI imaging) also showed microscale segregation of analytes within MALDI spots [49,50].

The occurrence of coffee-ring effect in MALDI raises discussion about the underlying mechanism. During the evaporation of matrix/sample droplet, several processes take place in parallel. Due to the outward capillary flow, the coffee-ring effect pins particles on the contact line, which is counteracted by the so-called "Marangoni effect". The latter arises because the differences in evaporation rates produce a surface tension gradient and induce a radial flow toward the center of the droplet. In fact, under certain conditions, the Marangoni effect may reverse the coffee-ring effect [56]. However, in the case of MALDI spots (Fig. 3), crystallization occurs simultaneously with particle transport (presumably governed by the two effects). Sequential partitioning of different metabolites to the precipitate can dictate their distribution within the spots. The analytes that partition to precipitate particles will be driven to the edge of the spot despite the presence of the Marangoni effect. Since the zones of different analytes are formed within the MALDI spots, a rough separation of analytes can be achieved.

3.3. An attempt to suppress coffee-ring effect in LDI-MS

Several methods to suppress the occurrence of the coffee-ring effect have been described in literature. They include modifying the composition of particle suspension [57–59], adjusting substrate temperature [56,60], or altering surface wettability [61–63]. For example, Mugele and co-workers pointed out that using electrowetting technology can inhibit coffee-ring effect and enhance the intensities of MALDI-MS signals [63]. Here we propose another simple method, which is compatible with the dried-droplet sample preparation in SALDI. It involves the use of a hydrophobic substrate. The sample target was an ITO glass slide coated with a hydrophobic layer of polysilazane. When deposited on such a slide, graphite powder did not pin to the hydrophobic surface and the suspension droplet contracted during the evaporation of solvent. This was followed by formation of a dry residue deposit (Fig. 4). The deposit had a small diameter (~750 μm) compared to the droplet size (~1400 μm) and did not exhibit formation of a coffee ring. We further applied this method to sample preparation in MALDI, however, in this case, the suppression of coffee rings was not as effective as in the case of graphite powder (data not shown). Overall, as

noted elsewhere [61,62], the coffee-ring effect can be suppressed by changing surface wettability, and under certain conditions, this strategy may be applicable to sample preparation in SALDI-MS.

It should be noted that the formation of a MALDI sample deposit is a much more complex process than deposition of a suspension of particles (as in the case of SALDI). Organic matrices precipitate due to a lowered solubility upon mixing with the sample solvent and continuous evaporation of solvents. The precipitate may initially undergo rearrangement according to the coffee-ring effect and the Marangoni effect. However, the suspension particles are promptly pinned to the surface, which is not only due to precipitation and evaporation of solvent but also due to the formation of crystalline junctions connecting individual crystals and the resulting immobilization on the surface. These processes are accompanied by adsorption, occlusion, and co-precipitation with analytes and other components of the samples, all of which are selective and contribute to the heterogeneous distribution of chemical species within the resulting deposits.

4. Conclusions

In the present work, distributions of analytes (phosphate metabolites) and matrices in MALDI and SALDI sample spots have been studied using optical/fluorescence microscopy, and MS imaging. In both cases, we have observed the occurrence of the coffee-ring effect. We argue that the coffee-ring effect plays two concurrent roles, which have advantages and disadvantages. The formation of the coffee rings is partly responsible for heterogeneous distribution of the analytes and the matrix, which compromises analytical performance and reproducibility. On the other hand, it enables a rough separation of the sample/matrix components. Coffee rings were observed even in the absence of inorganic or organic matrices. We also reported on a hidden coffee-ring effect in MALDI where under certain conditions the sample/matrix deposit appears homogeneous. Nevertheless, the coffee rings were still found by MALDI-MS imaging executed using dense laser raster scans. We found that to some extent, formation of coffee rings in SALDI could be suppressed by modifying the surface wettability.

Acknowledgments

We thank Ms Wei-Ru Ciou for her assistance with SEM and EDX, and Dr Jonathan Fang for correcting our manuscript. We acknowledge the National Science Council of Taiwan for the financial support.

Appendix A. Supplementary data

Supplementary data associated with this article can be found, in the online version, at http://dx.doi.org/10.1016/j.aca.2012.12.044.

References

[1] M. Karas, D. Bachmann, F. Hillenkamp, Anal. Chem. 57 (1985) 2935–2939.
[2] J. Sunner, E. Dratz, Y.-C. Chen, Anal. Chem. 67 (1995) 4335–4342.
[3] M.W.F. Nielen, Mass Spectrom. Rev. 18 (1999) 309–344.
[4] R. Arakawa, H. Kawasaki, Anal. Sci. 26 (2010) 1229–1240.
[5] C.-K. Chiang, W.T. Chen, H.-T. Chang, Chem. Soc. Rev. 40 (2011) 1269–1281.
[6] G. McCombie, R. Knochenmuss, J. Am. Soc. Mass Spectrom. 17 (2006) 737–745.
[7] D.W. Armstrong, L.-K. Zhang, L. He, M.L. Gross, Anal. Chem. 73 (2001) 3679–3686.
[8] A. Tholey, Rapid Commun. Mass Spectrom. 20 (2006) 1761–1768.
[9] R. Lemaire, J.C. Tabet, P. Ducoroy, J.B. Hendra, M. Salzet, I. Fournier, Anal. Chem. 78 (2006) 809–819.
[10] S.D. Hanton, D.M. Parees, J. Am. Soc. Mass Spectrom. 16 (2005) 90–93.
[11] S. Trimpin, T.N. Herath, E.D. Inutan, J. Wager-Miller, P. Kowalski, E. Claude, J.M. Walker, K. Mackie, Anal. Chem. 82 (2010) 359–367.
[12] M. Karas, F. Hillenkamp, Anal. Chem. 60 (1988) 2299–2301.
[13] F. Hillenkamp, J. Peter-Katalinić, MALDI MS. A Practical Guide to Instrumentation, Methods and Applications, Wiley–VCH, Germany, 2007, p. 119.
[14] A.L. Burlingame, R.K. Boyd, S.J. Gaskell, Anal. Chem. 70 (1998) 647–716.
[15] O. Vorm, P. Roepstorff, M. Mann, Anal. Chem. 66 (1994) 3281–3287.
[16] R.D. Deegan, O. Bakajin, T.F. Dupont, G. Huber, S.R. Nagel, T.A. Witten, Nature 389 (1997) 827–829.
[17] W. Han, Z. Lin, Angew. Chem. Int. Ed. 51 (2012) 1534–1546.
[18] N.C. Schirmer, S. Ströhle, M.K. Tiwari, D. Poulikakos, Adv. Funct. Mater. 21 (2011) 388–395.
[19] B.-J. Gans, U.S. Schubert, Langmuir 20 (2004) 7789–7793.
[20] R. Blossey, A. Bosio, Langmuir 18 (2002) 2952–2954.
[21] T.S. Wong, T.H. Chen, X.Y. Shen, C.M. Ho, Anal. Chem. 83 (2011) 1871–1873.
[22] C. Monteux, F. Lequeux, Langmuir 27 (2011) 2917–2922.
[23] K. Uetani, H. Yano, ACS Macro Lett. 1 (2012) 651–655.
[24] Y.-C. Chen, J.-Y. Wu, Rapid Commun. Mass Spectrom. 15 (2001) 1899–1903.
[25] Y.-C. Chen, M.-C. Sun, Rapid Commun. Mass Spectrom. 16 (2002) 1243–1247.
[26] T. Kinumi, T. Saisu, M. Takayama, H. Niwa, J. Mass Spectrom. 35 (2000) 417–422.
[27] W.-Y. Chen, Y.-C. Chen, Anal. Bioanal. Chem. 386 (2006) 699–704.
[28] Y.-C. Chiu, Y.-C. Chen, Anal. Lett. 41 (2008) 260–267.
[29] T. Watanabe, H. Kawasaki, T. Yonezawa, R. Arakawa, J. Mass Spectrom. 43 (2008) 1063–1071.
[30] Y.-C. Chen, J. Shiea, J. Sunner, Rapid Commun. Mass Spectrom. 14 (2000) 86–90.
[31] Y.-C. Chen, M.-F. Tsai, Rapid Commun. Mass Spectrom. 14 (2000) 2300–2304.
[32] Y.-C. Chen, M.-C. Sun, Rapid Commun. Mass Spectrom. 15 (2001) 2521–2525.
[33] C.-T. Chen, Y.-C. Chen, Anal. Chem. 77 (2005) 5912–5919.
[34] X.L. Kong, L.C.L. Huang, C.-M. Hsu, W.-H. Chen, C.-C. Han, H.-C. Chang, Anal. Chem. 77 (2005) 259–265.
[35] M.V. Ugarov, T. Egan, D.V. Khabashesku, J.A. Schultz, H. Peng, V.N. Khabashesku, H. Furutani, K.S. Prather, H.-W.J. Wang, S.N. Jackson, A.S. Woods, Anal. Chem. 76 (2004) 6734–6742.
[36] W.-Y. Chen, L.-S. Wang, H.-T. Chiu, Y.-C. Chen, C.-Y. Lee, J. Am. Soc. Mass Spectrom. 15 (2004) 1629–1635.
[37] J. Wei, J.M. Buriak, G. Siuzdak, Nature 399 (1999) 243–246.
[38] S. Okuno, R. Arakawa, K. Okamoto, Y. Matsui, S. Seki, T. Kozawa, S. Tagawa, Y. Wada, Anal. Chem. 77 (2005) 5364–5369.
[39] C.-T. Chen, Y.-C. Chen, Rapid Commun. Mass Spectrom. 18 (2004) 1956–1964.
[40] C.-T. Chen, Y.-C. Chen, Anal. Chem. 76 (2004) 1453–1457.
[41] K.-H. Lee, C.-K. Chiang, Z.-H. Lin, H.-T. Chang, Rapid Commun. Mass Spectrom. 21 (2007) 2023–2030.
[42] Y.-F. Huang, H.-T. Chang, Anal. Chem. 78 (2006) 1485–1493.
[43] Y.-F. Huang, H.-T. Chang, Anal. Chem. 79 (2007) 4852–4859.
[44] H. Kawasaki, T. Sugitani, T. Watanabe, T. Yonezawa, H. Moriwaki, R. Arakawa, Anal. Chem. 80 (2008) 7524–7533.
[45] Y.-S. Lin, Y.-C. Chen, Anal. Chem. 74 (2002) 5793–5798.
[46] K.-C. Ho, Y.-S. Lin, Y.-C. Chen, Rapid Commun. Mass Spectrom. 17 (2003) 2683–2687.
[47] W.-Y. Chen, Y.-C. Chen, Anal. Chem. 75 (2003) 4223–4228.
[48] C.-H. Teng, Y.-C. Chen, Rapid Commun. Mass Spectrom. 17 (2003) 1092–1094.
[49] S.L. Luxembourg, L.A. McDonnell, M.C. Duursma, X. Guo, R.M.A. Heeren, Anal. Chem. 75 (2003) 2333–2341.
[50] W. Bouschen, B. Spengler, Int. J. Mass Spectrom. 266 (2007) 129–137.
[51] H. Kawasaki, H. Yamamoto, H. Fujimori, R. Arakawa, M. Inada, Y. Iwasaki, Chem. Commun. 46 (2010) 3759–3761.
[52] J.-Y. Wu, Y.-C. Chen, J. Mass Spectrom. 37 (2002) 85–90.
[53] J. Zhang, Z. Li, C. Zhang, B. Feng, Z. Zhou, Y. Bai, H. Liu, Anal. Chem. 84 (2012) 3296–3301.
[54] H.-W. Tang, K.-M. Ng, W. Lu, C.-M. Che, Anal. Chem. 81 (2009) 4720–4729.
[55] T.R. Northen, O. Yanes, M.T. Northen, D. Marrinucci, W. Uritboonthai, J. Apon, S.L. Golledge, A. Nordström, G. Siuzdak, Nature 449 (2007) 1033–1037.
[56] H. Hu, R.G. Larson, J. Phys. Chem. B 110 (2006) 7090–7094.
[57] J. Park, J. Moon, Langmuir 22 (2006) 3506–3513.
[58] D. Kim, S. Jeong, B.K. Park, J. Moon, Appl. Phys. Lett. 89 (2006) 264101.
[59] R. Bhardwaj, X. Fang, P. Somasundaran, D. Attinger, Langmuir 26 (2010) 7833–7842.
[60] D. Soltman, V. Subramanian, Langmuir 24 (2008) 2224–2231.
[61] F.Q. Fan, K.J. Stebe, Langmuir 20 (2004) 3062–3067.
[62] H.Y. Ko, J. Park, H. Shin, J. Moon, Chem. Mater. 16 (2004) 4212–4215.
[63] D. Mampallil, H.B. Eral, D. van den Ende, F. Mugele, Soft Matter 8 (2012) 10614–10617.